

Journal of Materials Chemistry A

Accepted Manuscript



This is an *Accepted Manuscript*, which has been through the Royal Society of Chemistry peer review process and has been accepted for publication.

Accepted Manuscripts are published online shortly after acceptance, before technical editing, formatting and proof reading. Using this free service, authors can make their results available to the community, in citable form, before we publish the edited article. We will replace this *Accepted Manuscript* with the edited and formatted *Advance Article* as soon as it is available.

You can find more information about *Accepted Manuscripts* in the [Information for Authors](#).

Please note that technical editing may introduce minor changes to the text and/or graphics, which may alter content. The journal's standard [Terms & Conditions](#) and the [Ethical guidelines](#) still apply. In no event shall the Royal Society of Chemistry be held responsible for any errors or omissions in this *Accepted Manuscript* or any consequences arising from the use of any information it contains.



Journal Name

COMMUNICATION

Amorphous Co-doped MoS₂ nanosheets coated on metallic CoS₂ nanocubes as an excellent electrocatalyst for hydrogen evolution[†]

Received 00th January 20xx,
Accepted 00th January 20xx

Haichuan Zhang,^a Yingjie Li,^a Tianhao Xu,^a Jiabao Wang,^a Ziyang Huo,^b Pengbo Wan^a and Xiaoming Sun^{*a}

DOI: 10.1039/x0xx00000x

www.rsc.org/

The amorphous Co-doped MoS₂ coated on high-crystallized pyrite-phase CoS₂ hierarchical nanoarray exhibits ultrahigh activity towards acidic hydrogen evolution with a low onset potential (~44 mV) and a small overpotential of ~110.5 mV for driving the current density of ~10 mA cm⁻², ascribed to the novel hierarchical structure and the Co doping caused synergistic effects.

The generation of hydrogen, a sustainable, high-efficiency and clean next-generation alternative carbon-free energy carrier for replacing fossil fuels, has attracted extensive interest.¹⁻³ The most promising way to produce clean hydrogen fuel is water splitting by either light or electricity.⁴ Though Pt-group metals have been demonstrated as most effect catalysts for hydrogen evolution reaction (HER), the low-abundance and high-cost seriously limit the large-scale commercial application.^{5,6} It's vitally important to develop highly HER electrocatalytic active materials that are more earth-abundant and stable at lower costs, so that to pave the way for the hydrogen economy era.⁶

Nanostructured molybdenum sulfide materials have been most extensively investigated as promising non-precious electrocatalysts for hydrogen evolution, where the HER active sites were demonstrated lying in the edges of MoS₂ catalysts but not their basal planes.^{1, 7, 8} However, low conductivity, limited surface area, preferential exposure of the active sites and activation of the inactive edges for MoS₂ materials still remain challenging.^{1, 9-12} To address the above issues, considerable research efforts have therefore been placed on promotion of MoS₂ catalysts, with successful functional-design examples including core-shell MoO₃-MoS₂ nanowires,⁹ MoS₂/graphene hybrid materials,¹ transition-metal doped MoS₂ catalysts,¹³⁻¹⁵ N doped MoS₂ material¹⁶ and amorphous MoS₂ porous film¹¹. In spite of these progresses, it is still intriguing to search new and effective approaches which would offer extra/better options and

different ways of thinking to the functional design of MoS₂ catalysts. Recently, a number of transition metal dichalcogenides materials, such as CoS₂,^{6, 17} CoSe₂,^{5, 18} FeS₂,^{5, 17} and NiS₂,^{5, 17} which are low cost, earth-abundant and expected long-term stability in acidic operating environments, are explored for effective HER electrocatalysis. Among them, pyrite-phase CoS₂ has been widely recognized as a superb catalyst with a great advantage of intrinsically metal-like conductivity.^{6, 19, 20} Therefore, the appropriate integration of the highly active site with the partially metallic features would prompt the catalytic performance significantly and open up new opportunities for building up high performance electrodes in further.

Herein, we present a facile hydrothermal method to integrate the Co-doped MoS₂ nanosheets on the surface of metallic CoS₂ nanocubes (CoS₂@MoS₂), where a robust and effective hierarchical structure towards HER was demonstrated in particular. As a binder-free electrode, such CoS₂@MoS₂ hierarchical nanoarray with mesoporous surface exhibited excellent electrocatalytic activity, including onset potential as low as ~44 mV and low Tafel slope down to ~57.3 mV dec⁻¹. The high performance was attributed to the Co-doping into amorphous MoS₂, the unique hierarchical structure, the metallic property of pyrite-phase CoS₂ and tight/direct binding between catalysts and substrate, and further demonstrated the importance of constructing micro-/nano-structured electrodes and introducing transition metals into MoS₂ 2D structures.

The synthesis of CoS₂@MoS₂ hierarchical nanoarray was performed in simple hydrothermal conditions involving precipitation and sulfidation of CoCl₂ and (NH₄)₆Mo₇O₂₄ on a Ti substrate while thiourea (CS(NH₂)₂) was used as S source. After hydrothermal reaction, a pink-gray film (Fig. 1A) was formed on the originally bright Ti foil (Fig. S1) with intimate contact. The as-formed CoS₂ nanocubes with lateral size of several hundred nanometers were uniformly grown on Ti foil and densely coated by thin MoS₂ nanosheets, as revealed by SEM characterization (Fig. 1B). The growth process of CoS₂@MoS₂ hierarchical nanoarray was schematically illustrated in Fig. 1C, based on SEM observation. There are two main steps in the formation: metallic CoS₂ nanocubes growth and amorphous MoS₂ nanosheets coating. At the initial stage, there were only tiny nuclei formed on the Ti substrate in 3 hours (Fig.

^a State Key Laboratory of Chemical Resource Engineering, Beijing University of Chemical Technology, Beijing 100029, China. E-mail: sunxm@mail.buct.edu.cn

^b Queensland Micro- and Nanotechnology Centre Nathan campus, Griffith University, 170 Kessels Road, NATHAN QLD 4111, Australia.

[†] Electronic Supplementary Information (ESI) available: Detailed experimental procedure, optical and SEM images, polarization curves, EDLC measurements, table of HER performances, XRD patterns and Raman spectra. See DOI: 10.1039/x0xx00000x

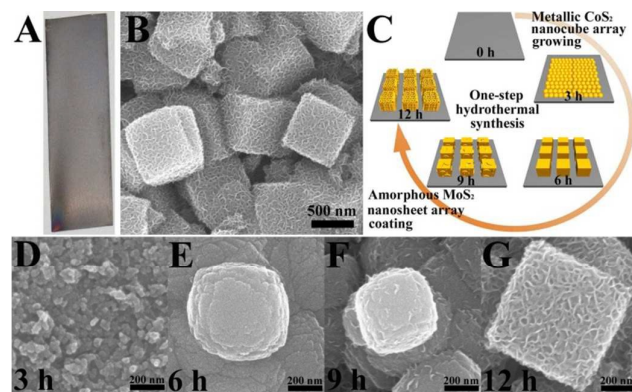


Fig. 1 (A) Optical image and (B) low-resolution SEM image of CoS_2 @ MoS_2 hierarchical nanoarray; (C) schematic illustration of the growth process of CoS_2 @ MoS_2 hierarchical nanoarray; (D, E, F and G) high-resolution SEM images of CoS_2 @ MoS_2 hierarchical nanoarray obtained for the reaction time at 3h, 6h, 9h and 12h.

1D), while they grew into roughly cubic microstructures in 6 hours (Fig. 1E). Secondary growth of nanosheets on the submicrometer sized cubes started at the timepoint of 9 hours (Fig. 1F), and in the consequent 3 hours (12 hrs), the cubes fully grew into edge-sharp morphologies with uniform MoS_2 coating all throughout (Fig. 1G). By sharing the same sulphur precursor (thiourea) and manipulating growth kinetics, the successful combination of materials synthesis and dopant has been realized in a single step, which could be extendable to other hierarchical nanostructures.

The CoS_2 @ MoS_2 hierarchical nanoarray material was fully characterized by X-ray diffraction (XRD), Raman spectrum, high-resolution transmission electron microscopy (HRTEM) and X-ray photoelectron spectrum (XPS). As shown in Fig. 2A, all peaks in the XRD patterns were sharp, which were assigned to pyrite-phase CoS_2 (JCPDS No. 41-1471) and Ti substrate (No. 65-9622),¹⁹ which suggested the good crystallinity of CoS_2 and amorphous nature of MoS_2 . The Raman spectrum (Fig. 2B) from CoS_2 @ MoS_2 sample showed characteristic peaks at ~ 288 and ~ 394 cm^{-1} for CoS_2 and the A_{1g} mode at ~ 414 cm^{-1} for MoS_2 , evidencing the formation of MoS_2 .^{10, 21-24} The binding energy of the Mo $3d_{5/2}$ electron peak at 229.5 eV (Fig. S2B) revealed the +4 oxidation state of Mo element, further confirming the formation of MoS_2 .^{9, 11} The HRTEM image in Fig. 2C clearly showed the existence of crystal boundary and tight binding between the high-crystallized CoS_2 nanocubes and amorphous MoS_2 nanosheets, revealing the advantage of one-step hydrothermal synthesis. And the lattice fringe with interplanar spacing of ~ 0.554 nm arose from twice the (200) plane of pyrite-phase CoS_2 . The HRTEM image (Fig. 2D and S3) recorded on amorphous MoS_2 coating further demonstrated its layered but amorphous structure, by showing interlayer distance of ~ 0.615 nm. Elemental mapping using STEM on the conjugated zone of CoS_2 and MoS_2 (Fig. 2E) confirmed the intimate contact between CoS_2 and MoS_2 by showing homogeneous S element distribution, and more importantly, revealed the co-existence of Co element with MoS_2 , in spite of the relatively low-content as compared with CoS_2 (the bright zone in Co mapping data), indicating the Co-doping of MoS_2 .

The CoS_2 @ MoS_2 layer on Ti substrate serves as a binder-free catalyst for electrochemical studies. For comparison, the HER

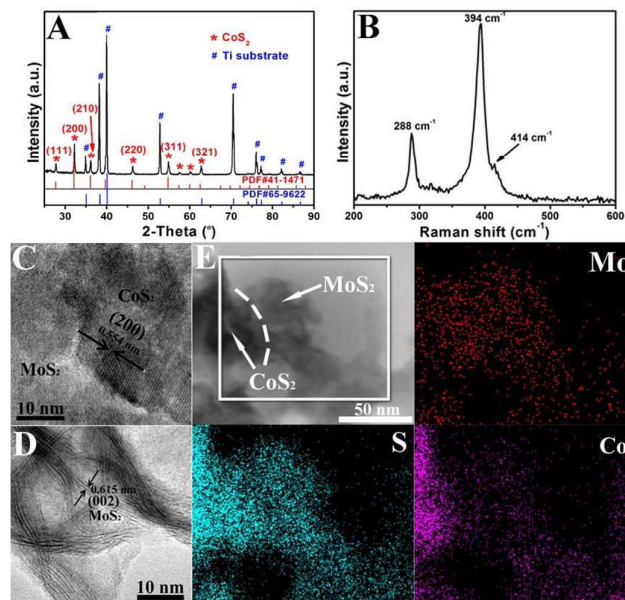


Fig. 2 (A) XRD pattern, (B) Raman spectrum, (C and D) high-resolution TEM images and (E) elemental mapping of CoS_2 @ MoS_2 hierarchical nanoarray.

activities of all the as-prepared electrocatalysts, including CoS_2 nanopyramids (SEM images in Fig. S4A and S4B), MoS_2 nanosheets (SEM images in Fig. S4C and S4D) and CoS_2 @ MoS_2 hierarchical nanoarray, were investigated in a typical three-electrode cell setup with 0.5 M H_2SO_4 electrolyte, and Pt electrode was used as control. The IR-corrected polarization curves in Fig. 3A (measured current normalized by the geometrical area of the electrode and corrected by the solution resistance in Fig. 3B, and uncorrected polarization curves in Fig. S5) showed that the CoS_2 @ MoS_2 electrocatalyst exhibited much higher HER performance than CoS_2 nanopyramid array and MoS_2 nanosheet array. Using the overpotential at 10 mA cm^{-2} as standard, the CoS_2 @ MoS_2 sample is 68 mV higher than Pt, but 83 mV smaller than CoS_2 nanoarray, and 115 mV better than MoS_2 nanoarray. A very small onset potential (~ 44 mV) is observed based on the Tafel curve as shown in Fig. 3C, which was mainly attributed to the synergistic effect of Co-doping into amorphous MoS_2 nanosheets, which further enrich the defect structure and activated some unreactive edge sites.^{11, 13, 14} An overpotential as low as ~ 110 mV was enough to generate HER cathodic current density to ~ 10 mA cm^{-2} for the CoS_2 @ MoS_2 electrode, which is among the best record on sulphide-based HER electrodes.^{4, 6, 9, 19}

The overwhelming performance of CoS_2 @ MoS_2 hierarchical nanoarray for HER than CoS_2 nanopyramid array and MoS_2 nanosheet array, could also be beneficial from the better electron transportation and higher electrochemically active surface area (ECSA). Obviously, as shown in the Nyquist plots (Fig. 3B), the reaction resistance for CoS_2 @ MoS_2 electrode is the smallest, less than 1 Ω , while the MoS_2 electrode associated with poor conductivity displays the largest charge transfer resistance. Available electrochemical approach to estimate the effective ECSA of the solid-liquid interfaces is to measure the electrochemical double-layer capacitance (EDLC) extracted from the capacitive current as a function of scan rate.²⁵⁻²⁷ The EDLC values of CoS_2 @ MoS_2

nanoarray, MoS₂ nanosheet array and CoS₂ nanopyramid array, as

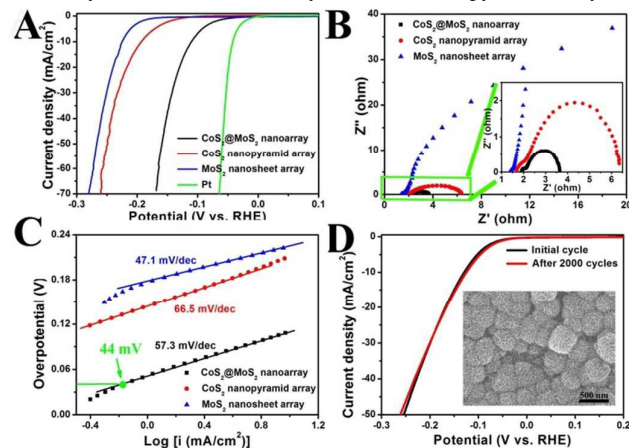


Fig. 3 (A) IR-corrected polarization curves, (B) Nyquist plots, (C) Tafel plots of several electrocatalysts as indicated, including CoS₂@MoS₂ hierarchical nanoarray, CoS₂ nanopyramid array and MoS₂ nanosheet array, and (D) polarization curves of CoS₂@MoS₂ hierarchical nanoarray electrode initially and after 2000 CV cycles between 0.2 and -0.3V vs. RHE. The inset is the corresponding SEM image of CoS₂@MoS₂ hierarchical nanoarray after the 2000 CV cycles durability test.

shown in Fig. S6, were 12.03, 8.78 and 4.86 mF cm⁻², respectively, which indicated that CoS₂@MoS₂ had the largest effective electrochemical area, which implied more active sites. Combining hierarchical structure and high surface area, as well as the Co-doping effect on MoS₂, the CoS₂@MoS₂ hierarchical nanoarray showed the best HER performance.

The CoS₂@MoS₂ electrocatalyst was further evaluated by comparing the HER performance with MoS₂ or CoS₂ electrocatalysts in acidic media from the related literatures (Table S1).^{4, 6, 9, 13, 17, 19} It was revealed that the CoS₂@MoS₂ hierarchical nanoarray possesses significantly higher HER activity than the catalysts reported previously.^{4, 6, 9, 13} Such higher HER electrocatalytic performance of the CoS₂@MoS₂ hierarchical nanoarray material could be rationalized as follows: (1) the intimate contact among Ti foil, CoS₂ and MoS₂, due to one-step hydrothermal synthesis, accelerates electron transport from substrate to catalyst layer during hydrogen evolution; (2) the high-crystallized pyrite-phase CoS₂, as a metallic material with good conductivity,^{6, 20} also facilitates the carrier flow from the nanocubes to MoS₂ nanosheets; (3) the hierarchical structure of CoS₂@MoS₂ nanoarray with increased effective surface area offers abundant active sites to promote the HER performance; (4) the porosity of hierarchical structure benefits the diffusion of the electrolyte into all the pores and thus more efficient use of active sites in CoS₂ and MoS₂; (5) the amorphous structure of MoS₂ produces abundant defect sites as HER electrocatalytic active sites;^{11, 13} (6) the S-edges of MoS₂ activated by Co-doping possess electrocatalytic activity to enhance the HER performance.¹³⁻¹⁵

Stability is another very important criterion in evaluating electrocatalysts for commercial applications.^{3, 9} The durability of the CoS₂@MoS₂ electrocatalyst in an acidic environment was performed by taking continuous cyclic voltammograms at an accelerated scanning rate of ~30 mV s⁻¹ for 2000 cycles. As shown in Fig. 3D, no obvious decay of the activity is observed based on the

polarization curves before and after 2000 cycles, which could be attributed to the tight binding between the active material and substrate by the one-step hydrothermal method. The SEM image of CoS₂@MoS₂ hierarchical nanoarray after cycling (the inset of Fig. 3D) shows essentially the same surface structure, further confirming the robustness of the electrode. And the adhesive force as low as ~9.31 μN for the CoS₂@MoS₂ electrode (Fig. S7) benefits the release of as-formed H₂ bubbles and the stability of the surface of electrode.^{3, 4} As displayed in Fig. S8, S9 and S10, the XRD patterns, Raman spectra and XPS spectra with no phase changes as a result of HER electrocatalysis demonstrate the chemical stability of CoS₂@MoS₂ grown on Ti foil. To probe long-term stability under acidic condition, the CoS₂@MoS₂ material was assessed over 15 hours under a constant potential. It's worth noting that, as shown in Fig. S11, the current density has retained almost 93.5% after the 15-h testing, suggesting the great potential of replacing noble metals used in practical applications for hydrogen evolution.

Conclusions

The CoS₂@MoS₂ hierarchical nanoarray, as a non-noble metal cathodic HER electrocatalyst in acidic environment, were directly grown on Ti foil via a simple and facile hydrothermal method. The CoS₂@MoS₂ electrode exhibited ultrahigh HER activity, and worked extremely stable after 2000 cycles. The excellent performance could be ascribed to the novel hierarchical structure, tight binding between catalysts and substrate, metallic property of pyrite-phase CoS₂ and intrinsically electrocatalytic activity of amorphous Co-doped MoS₂. The fabrication of earth-abundant-based hierarchical nanoarray materials could inspire the functional design of other related hierarchical electrodes which are potential ready for practical applications.

This work was supported by National Natural Science Foundation of China, 973 Program (2011CBA00503, 2011CB932403), the Program for Changjiang Scholars and Innovative Research Team in the University, and the Fundamental Research Funds for the Central Universities.

Notes and references

1. Y. Li, H. Wang, L. Xie, Y. Liang, G. Hong and H. Dai, *J. Am. Chem. Soc.*, 2011, **133**, 7296-7299.
2. J. K. Norskov, T. Bligaard, J. Rossmeisl and C. H. Christensen, *Nat Chem*, 2009, **1**, 37-46.
3. Y. Li, H. Zhang, T. Xu, Z. Lu, X. Wu, P. Wan, X. Sun and L. Jiang, *Adv. Funct. Mater.*, 2015, **25**, 1737-1744.
4. Z. Lu, W. Zhu, X. Yu, H. Zhang, Y. Li, X. Sun, X. Wang, H. Wang, J. Wang, J. Luo, X. Lei and L. Jiang, *Adv. Mater.*, 2014, **26**, 2683-2687.
5. D. Kong, J. J. Cha, H. Wang, H. R. Lee and Y. Cui, *Energy Environ. Sci.*, 2013, **6**, 3553-3558.

COMMUNICATION

Journal Name

6. M. S. Faber, R. Dzedzic, M. A. Lukowski, N. S. Kaiser, Q. Ding and S. Jin, *J. Am. Chem. Soc.*, 2014, **136**, 10053-10061.
7. T. F. Jaramillo, K. P. Jorgensen, J. Bonde, J. H. Nielsen, S. Horch and I. Chorkendorff, *Science*, 2007, **317**, 100-102.
8. B. Hinnemann, P. G. Moses, J. Bonde, K. P. Jorgensen, J. H. Nielsen, S. Horch, I. Chorkendorff and J. K. Nørskov, *J. Am. Chem. Soc.*, 2005, 5308-5309.
9. Z. Chen, D. Cummins, B. N. Reinecke, E. Clark, M. K. Sunkara and T. F. Jaramillo, *Nano Lett.*, 2011, **11**, 4168-4175.
10. D. Kong, H. Wang, J. J. Cha, M. Pasta, K. J. Koski, J. Yao and Y. Cui, *Nano Lett.*, 2013, **13**, 1341-1347.
11. Z. Lu, H. Zhang, W. Zhu, X. Yu, Y. Kuang, Z. Chang, X. Lei and X. Sun, *Chem. Commun.*, 2013, **49**, 7516-7518.
12. Y. Yan, B. Xia, N. Li, Z. Xu, A. Fisher and X. Wang, *J. Mater. Chem. A*, 2015, **3**, 131-135.
13. D. Merki, H. Vrubel, L. Rovelli, S. Fierro and X. Hu, *Chem. Sci.*, 2012, **3**, 2515-2525.
14. H. Wang, C. Tsai, D. Kong, K. Chan, F. Abild-Pedersen, J. K. Nørskov and Y. Cui, *Nano Res.*, 2015, **8**, 566-575.
15. J. Bonde, P. G. Moses, T. F. Jaramillo, J. K. Nørskov and I. Chorkendorff, *Faraday Discuss.*, 2008, 219-231.
16. W. Zhou, D. Hou, Y. Sang, S. Yao, J. Zhou, G. Li, L. Li, H. Liu and S. Chen, *J. Mater. Chem. A*, 2014, **2**, 11358-11364.
17. M. S. Faber, M. A. Lukowski, Q. Ding, N. S. Kaiser and S. Jin, *J Phys Chem C*, 2014, **118**, 21347-21356.
18. D. Kong, H. Wang, Z. Lu and Y. Cui, *J. Am. Chem. Soc.*, 2014, **136**, 4897-4900.
19. H. Zhang, Y. Li, G. Zhang, P. Wan, T. Xu, X. Wu and X. Sun, *Electrochim. Acta*, 2014, **148**, 170-174.
20. H. Zhang, Y. Li, G. Zhang, T. Xu, P. Wan and X. Sun, *J. Mater. Chem. A*, 2015, **3**, 6306-6310.
21. R. Wei, H. Yang, K. Du, W. Fu, Y. Tian, Q. Yu, S. Liu, M. Li and G. Zou, *Mater. Chem. Phys.*, 2008, **108**, 188-191.
22. L. Zhu, D. Susac, M. Teo, K. Wong, P. Wong, R. Parsons, D. Bizzotto, K. Mitchell and S. Campbell, *J. Catal.*, 2008, **258**, 235-242.
23. I. Wiesel, H. Arbel, A. Albu-Yaron, R. Popovitz-Biro, J. M. Gordon, D. Feuermann and R. Tenne, *Nano Res.*, 2010, **2**, 416-424.
24. H. Zhou, F. Yu, Y. Liu, X. Zou, C. Cong, C. Qiu, T. Yu, Z. Yan, X. Shen, L. Sun, B. I. Yakobson and J. M. Tour, *Nano Res.*, 2013, **6**, 703-711.
25. S. Trasatti and O. A. Petrii, *J. Electroanal. Chem.*, 1992, 353-376.
26. C. C. McCrory, S. Jung, J. C. Peters and T. F. Jaramillo, *J. Am. Chem. Soc.*, 2013, **135**, 16977-16987.
27. W. Zhou, J. Zhou, Y. Zhou, J. Lu, K. Zhou, L. Yang, Z. Tang, L. Li and S. Chen, *Chem. Mater.*, 2015, **27**, 2026-2032.

Table of Contents

Amorphous Co-doped MoS₂ nanosheets coated on metallic CoS₂ nanocubes with ultrahigh HER activity were prepared via one-pot hydrothermal synthesis.

